# Supplemental material for: Subdiffusion and heat transport in a tilted 2D Fermi-Hubbard system

Elmer Guardado-Sanchez,* Alan Morningstar,* Benjamin M. Spar, Peter T. Brown, David A. Huse, and Waseem S. Bakr†
*Department of Physics, Princeton University, Princeton, New Jersey 08544 USA*
(Dated: November 25, 2019)

The experimental setup and basic parameters are already described in detail in the supplement of Ref. [1]. The spatial light modulator calibration is also explained in the supplement of Ref [2].

### Tilt potential calibration

To calibrate the gradient and characterize its homogeneity across the region of interest, we used the SLM to prepare an initial state consisting of three thin stripes of width $\sim 1\, a_{\mathrm{latt}}$ and a separation of $\sim 20\, a_{\mathrm{latt}}$, with their long direction oriented orthogonal to the tilt direction. Each stripe consists of a spin-polarized gas of the lowest hyperfine ground state of $^6$Li.

For weak tilts, we are able to directly measure Bloch oscillations of these non-interacting particles. We do so by fitting a Gaussian profile to the density profile integrated along the direction perpendicular to the tilt which is used to quantify the "breathing" oscillation of the width of the stripes. This is similar to what was done in [3]. From the theory of Bloch oscillations, we expect the width of each stripe to oscillate with a maximal half-width of $A = 4t_h/F$ and a period of $T = h/Fa_{\mathrm{latt}}$. Thus, by fitting a sinusoid to the evolution of the width of each stripe, we can extract the tilt strength at their respective positions. Fig. S1(a) shows an example of such oscillations.

For stronger tilts, directly measuring the Bloch oscillations becomes challenging due to their small amplitude. Instead we use a modulation technique analogous to what was done in [4]. We modulate the lattice potential at frequencies on the order of the tilt strength. This brings lattice sites that were decoupled due to the tilt into resonance which results in photon-assisted tunneling. We again measure the width of the thin stripes versus modulation frequency and observe a broadening of the stripes at resonance. Fig. S1(b) shows an example of such a measurement.

We corroborated that for the same potential strength at intermediate tilts, the gradient extracted using the two techniques agrees.

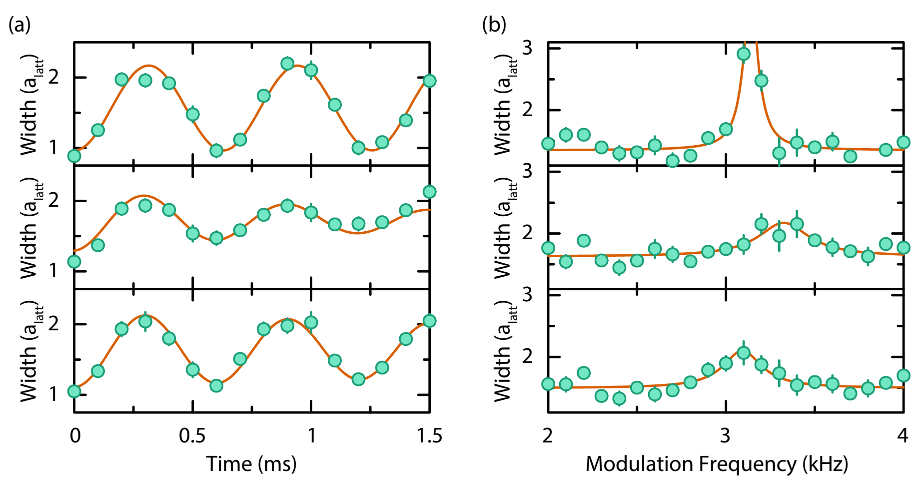


FIG. S1. **Tilt potential calibration.** (a) Bloch oscillation method for characterization of tilt strengths. Each graph corresponds to a measurement of the local gradient at the position of one of the three stripes. The measured tilt strength is $Fa_{\mathrm{latt}} = h \times 1.64(3)$ kHz with a maximal difference of 4.6% between stripes. (b) Lattice modulation method for characterization of tilt strengths. The measured tilt strength is $Fa_{\mathrm{latt}} = h \times 3.19(7)$ kHz with a maximal difference of 7.5% between stripes.

---

* These authors contributed equally to this work.

† Corresponding author. Email: wbakr@princeton.edu

### Linear response

Our hydrodynamic model assumes linearity in the amplitude of the initial inhomogeneities. In this experiment, we worked with relatively large amplitude density modulations. In a previous study ([2]), we worked with very small amplitude modulations and fit to a linear hydrodynamic model we developed. In the "tilted" system studied in this work, we are no longer working close to a ground state, and as such, the strength of the modulation is not expected to be as important.

Fig. S2 shows a comparison between the decay of strong and weak density modulations in a tilted potential. We observe that when we normalize the sinusoid amplitude and look at its decay, there is no measurable difference between the decays within the errorbars. This justifies working with strong modulations in this work to reduce the statistical error in the measurements for a fixed number of repetitions.

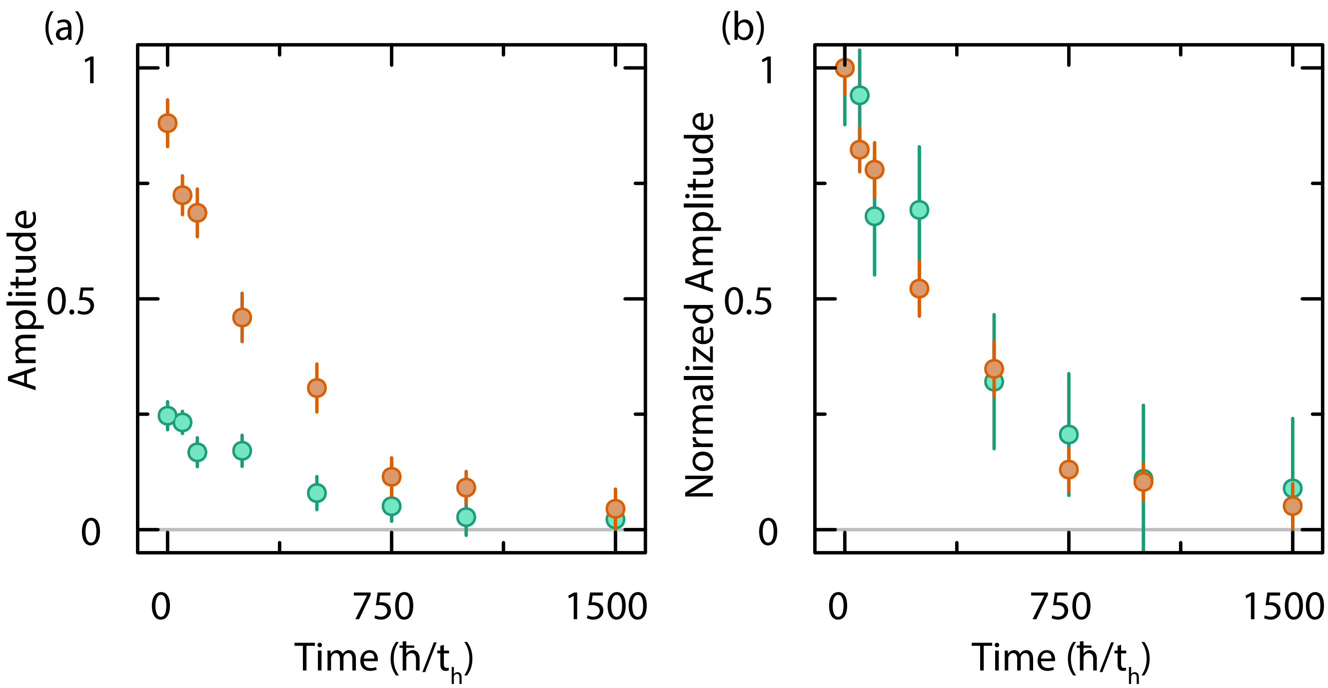


FIG. S2. **Test of linear response.** Decay of the amplitude of the density modulation *vs.* time for two different initial amplitudes of the modulation. Here $\lambda = 11.46(3)a_{\mathrm{latt}}$, $Fa_{\mathrm{latt}}/t_h = 6.1(2)$ and $U/t_h = 3.9(1)$. (a) Shows the amplitudes. (b) Shows the amplitudes normalized to the baseline at $t = 0$.

### Bulk shift

In the main text we focused on the late-time decay of the amplitude of initial density modulations and not on any early-time average local heating due to a bulk shift (phase slip) of the system along the tilted direction. We argued that the shift of the COM of the system cannot be more than $\sim (t_h + U)/F$ due to energy conservation and the finite kinetic and interaction energy densities that are possible in the system. In Fig. S3 we show measurements of the bulk shift of the COM as a function of time for a system with a relatively small tilt so that the bulk shift is appreciable. On a timescale $\sim 5\ \hbar/t_h$ the bulk shift reaches a steady state value and the system stops heating up.

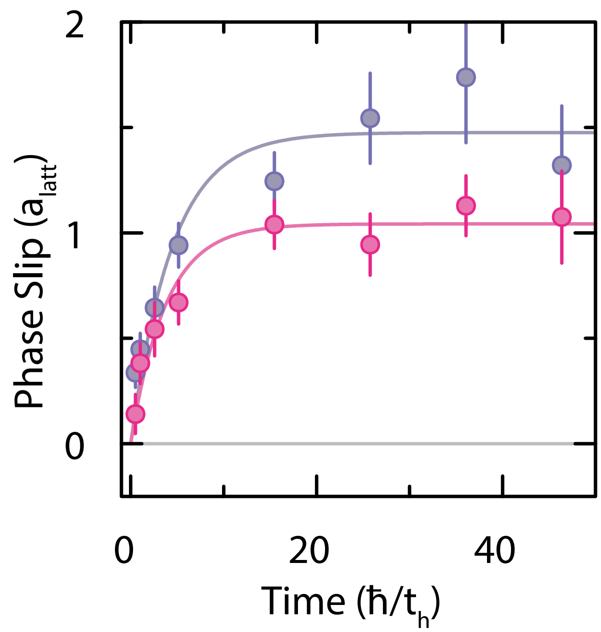


FIG. S3. **Phase slip.** The extracted phase slip (converted to units of lattice spacings) from the sinusoid fit to density profiles (circles) versus time. For wavelengths 19.33(7) $a_{\text{latt}}$ (purple) and 23.3(2) $a_{\text{latt}}$ (pink) at a tilt of $F/t = 0.99(3)$. The lines are exponential fits intended to guide the eye. After the early-time phase slip, the phase of the sinusoidal fit remains constant within error bars. Errorbars increase with time as the amplitude decays and the fit is less effective at determining the phase.

### Complete hydrodynamic model

We write our hydrodynamic theory in terms of the particle number density $n(x,t)$ and nontilt energy density $e(x,t)$, as well as their corresponding currents $j_n(x,t)$ and $j_e(x,t)$. Total particle number and total energy are conserved, and these conservation laws can be written as

$$\dot{n} + \nabla \cdot j_n = 0 \tag{S1}$$

$$\dot{e} + \nabla \cdot j_e - F j_n = 0. \tag{S2}$$

The entropic "force" laws that describe how currents are driven in this system are of the form $j_e = M_e \chi_e + M_{ne} \chi_n$ and $j_n = M_n \chi_n + M_{en} \chi_e$, where $\chi_e$ and $\chi_n$ are the entropic forces determined by the profiles of $e$ and $n$, and we insist on writing the forces in a "canonical basis" for which Onsager's reciprocal relations take the simple form $M_{en} = M_{ne}$. The $M$ coefficients are dynamical coefficients that are, in general, difficult to determine from the microscopic model. The off-diagonal coefficient $M_{ne}$ is associated with thermopower-type effects in our system, thus this model is quite general aside from its assumption of linearity, which is well-supported by our experimental measurements. In this canonical basis, the force $\chi_e$ is determined by the local change of entropy when an infinitesimal current of nontilt energy flows but no particle current flows. The force $\chi_n$ is determined in a similar fashion, with an infinitesimal particle current and no nontilt energy current, but note that if an infinitesimal particle current flows, then due to energy conservation there must be a production (or depletion) of nontilt energy. Thus the forces in this system take the form

$$\chi_e = \nabla \left( \frac{\partial s}{\partial e} \right) \tag{S3}$$

$$= -s_{ee} \nabla e + s_{ne} \nabla n \tag{S4}$$

$$\chi_n = \nabla \left( \frac{\partial s}{\partial n} \right) + F \left( \frac{\partial s}{\partial e} \right) \tag{S5}$$

$$= -s_{nn} \nabla n + s_{ne} \nabla e - s_{ee} F (e - \bar{e}(\bar{n})) + s_{ne} F (n - \bar{n}), \tag{S6}$$

where $s$ is the entropy density of the Fermi-Hubbard model, and we have expanded this entropy density near infinite-temperature equilibrium with $n = \bar{n}$ and $e = \bar{e}(\bar{n})$. The coefficients $s_{ee}$, $s_{nn}$, and $s_{ne}$ come from this high-temperature expansion:

$$s \approx s(\bar{n}, \bar{e}(\bar{n})) + s_n(n-\bar{n}) - \frac{1}{2}s_{nn}(n-\bar{n})^2 + s_{ne}(n-\bar{n})(e-\bar{e}(\bar{n})) - \frac{1}{2}s_{ee}(e-\bar{e}(\bar{n}))^2, \tag{S7}$$

and we emphasize that these coefficients are known functions of $U$, $t_h$ and $\bar{n}$ for the Fermi-Hubbard model.

Now that we have specified our model, we proceed in determining its eigenmodes and respective relaxation rates, with a particular focus on the slowest mode, which is representative of the late-time behavior that we analyze in the main text. To do this, we first organize our model into a matrix eigenvalue problem. The eigenmodes are functions of definite wavelength $\lambda$, and they decay to equilibrium at a rate $\tau^{-1}$, i.e. $e(x,t) - \bar{e}(\bar{n}) = \mathrm{e}^{-\Gamma t}(a\cos kx + b\sin kx)$ and $n(x,t) - \bar{n} = \mathrm{e}^{-\Gamma t}(c\cos kx + d\sin kx)$, where $k = 2\pi/\lambda$ and $\Gamma = 1/\tau$. We therefore write the above deviations of $e$ and $n$ from global equilibrium as $\boldsymbol{\rho} = (a\ b\ c\ d)^T$ in the basis $\{\mathrm{e}^{-\Gamma t}\cos kx, \mathrm{e}^{-\Gamma t}\sin kx, \mathrm{e}^{-\Gamma t}\cos kx, \mathrm{e}^{-\Gamma t}\sin kx\}$. In this language the currents are driven according to $\boldsymbol{j} = MU\boldsymbol{\rho}$ and the conservation laws are written as $-\Gamma\boldsymbol{\rho} = -\tilde{\nabla}\boldsymbol{j}$, where

$$U = \begin{pmatrix} 0 & -s_{ee}k & 0 & s_{ne}k \\ s_{ee}k & 0 & -s_{ne}k & 0 \\ -s_{ee}F & s_{ne}k & s_{ne}F & -s_{nn}k \\ -s_{ne}k & -s_{ee}F & s_{nn}k & s_{ne}F \end{pmatrix}, \quad M = \begin{pmatrix} M_e & 0 & M_{ne} & 0 \\ 0 & M_e & 0 & M_{ne} \\ M_{ne} & 0 & M_n & 0 \\ 0 & M_{ne} & 0 & M_n \end{pmatrix}, \quad \tilde{\nabla} = \begin{pmatrix} 0 & k & -F & 0 \\ -k & 0 & 0 & -F \\ 0 & 0 & 0 & k \\ 0 & 0 & -k & 0 \end{pmatrix}. \tag{S8}$$

Thus our model is solved via the eigenvalue problem $\Gamma\boldsymbol{\rho}_\Gamma = \tilde{\nabla}MU\boldsymbol{\rho}_\Gamma$. There are two solutions for $\Gamma$, each with a multiplicity of two corresponding to pure cos and sin waves for $n(x,t) - \bar{n}$. The only solution we need to consider at late times is the slow mode with $\Gamma = \Gamma_-$ and $n(x,t) - \bar{n} \propto \cos kx$. This eigenmode is representative of the dynamics of all monochromatic initial conditions at late times. In what follows we discuss some important features of the slowest eigenmode.

In the limit of small $F$ (and/or large $k$) the slowest mode is diffusive, i.e. $\Gamma \propto k^2$. In the limit of large $F$ (and/or small $k$) the slowest decay rate is

$$\Gamma_- \approx \frac{D_{\mathrm{th}}}{F^2}\left(\frac{s_{nn}}{s_{ee}} - \frac{s_{ne}^2}{s_{ee}^2}\right)k^4, \tag{S9}$$

where $D_{\mathrm{th}} = \left(M_e - (M_{ne}^2/M_n)\right)s_{ee}$ is the thermal diffusivity, and we will discuss why we identify it as such below. Thus we see that our model crosses over from diffusive to subdiffusive with $\tau \propto \lambda^4$ as $1/F\lambda$ becomes small.

If we assume a scaling of the form $\Gamma_- \propto k^\alpha$ we can estimate the exponent $\alpha$ by $\alpha = \frac{d\log\Gamma_-}{d\log k}\Big|_{k=k_e}$ evaluated at some $k$ in the experimental range $k \in [2\pi/24, 2\pi/12]$ denoted $k_e$. The general expression for $\alpha$ evaluated this way depends on the dynamical coefficients $M$, but in the limit where $\frac{M_e}{M_n}, \frac{M_{ne}}{M_n} \ll \frac{s_{nn}}{s_{ee}}$ this dependence drops out and we get a parameter-free estimate of $\alpha$ as a function of $F$. In this limit

$$\alpha(F) = 2 + \frac{2}{1 + \frac{s_{nn}}{s_{ee}}\frac{k_e^2}{F^2}}, \tag{S10}$$

and this is the theoretical estimate of $\alpha(F)$ that we use to compare to experimental results in the main text (Fig. 3 of main text).

Now we examine the structure of the slowest eigenmode itself and explain why we identify $D_{\mathrm{th}}$ as mentioned above. At small $k/F$, to leading order, the slowest eigenmode has

$$\boldsymbol{\rho}_{\Gamma_-} = \begin{pmatrix} \frac{s_{ne}}{s_{ee}} \\ \left(\frac{s_{nn}}{s_{ee}} - \frac{s_{ne}^2}{s_{ee}^2}\right)\frac{k}{F} \\ 1 \\ 0 \end{pmatrix}, \quad \boldsymbol{j}_{\Gamma_-} = \begin{pmatrix} -\left(M_e - \frac{M_{ne}^2}{M_n}\right)s_{ee}\left(\frac{s_{nn}}{s_{ee}} - \frac{s_{ne}^2}{s_{ee}^2}\right)\frac{k^2}{F} \\ \left(M_e - \frac{M_{ne}^2}{M_n}\right)s_{ne}\left(\frac{s_{nn}}{s_{ee}} - \frac{s_{ne}^2}{s_{ee}^2}\right)\frac{k^3}{F^2} \\ 0 \\ -\left(M_e - \frac{M_{ne}^2}{M_n}\right)s_{ee}\left(\frac{s_{nn}}{s_{ee}} - \frac{s_{ne}^2}{s_{ee}^2}\right)\frac{k^3}{F^2} \end{pmatrix}. \tag{S11}$$

We see that in this mode a modulation of number density with amplitude $\mathcal{O}(1)$ comes with a slow subdiffusive number density current $j_n \propto k^3$ that is "out of phase" by a quarter wavelength. This number current converts tilt energy to nontilt energy and this generates a small out of phase, nontilt energy profile with amplitude $\propto k/F$. That nontilt energy diffuses and we see that the ratio of amplitudes of the resulting "in phase" (with $n(x,t)$) energy current to the energy profile it is depleting is $|j_e|/|e| = D_{\mathrm{th}}k$ with $D_{\mathrm{th}} = \left(M_e - (M_{ne}^2/M_n)\right)s_{ee}$ as mentioned earlier. This is why we identify $D_{\mathrm{th}}$ as such. The process of diffusing the nontilt energy that is generated by the particle current that is relaxing the density profile is the bottleneck process and obeys a diffusion equation with diffusivity $D_{\mathrm{th}}$. That is why this diffusivity shows up as the one unknown coefficient in $\Gamma_-$, and thus we use our data to determine it in the regime where $\tau \propto \lambda^4$ where this mechanism is valid.

Now let's address the $\beta$ profile in this mode. The "in phase" component of $e - \bar{e}(\bar{n})$ shown in Eqn. S11, which is larger than the out of phase component by a factor of $F/k$, is due to the difference between $\bar{e}(\bar{n})$ and $\bar{e}(n)$, and not due to a nonzero $\beta$ component that is in phase. Since $\beta$ is proportional to $e - \bar{e}(n)$ at high temperatures, to leading order in the high-temperature limit $\beta(x,t)$ is set by the out of phase component of $e - \bar{e}(n)$ which is the same as $e - \bar{e}(\bar{n})$ for that component because the out of phase component of $n - \bar{n}$ is zero by definition (since "in phase" and "out of phase" are defined relative to the $n(x,t)$ profile here). Thus this model predicts an out of phase local $\beta$ modulation with amplitude

$$\mathrm{amp}(\beta(x,t)) = -s_{ee}\left(\frac{s_{nn}}{s_{ee} - \frac{s_{ne}^2}{s_{ee}^2}}\right)\frac{k}{F} \tag{S12}$$

$$= \frac{1}{\bar{n}\left(1 - \frac{\bar{n}}{2}\right)}\frac{k}{F}, \tag{S13}$$

where we have used the high temperature expressions for $s_{ee}$, $s_{ne}$, and $s_{nn}$. Indeed in the main text we show measurements of the local $\beta$ that are consistent with this prediction (Fig. 5 of main text). We call the nontilt energy current that results from this local $\beta$ profile the "heat current" $j_h$. Thus $D_{\mathrm{th}}$ is the diffusivity corresponding to the heat current that is being driven by the nontilt energy that is generated by the relaxation of the particle number distribution.

## High temperature expansion

We compute the grand partition function of the Fermi-Hubbard model in the high temperature expansion to second order in $\beta$ and evaluate the second partial derivatives of the entropy density with respect to $n$, the particle number density, and $e$, the energy density due to $t_h$ and $U$ terms, in order to compute the coefficients $s_{ee}$, $s_{nn}$, $s_{ne}$, and $s_n$. The results are

$$s_n = -\beta\mu \tag{S14}$$

$$s_{ee} = \frac{16}{\bar{n}(2-\bar{n})(32t_h^2 + \bar{n}(2-\bar{n})U^2)} \tag{S15}$$

$$s_{nn} = \frac{64t_h^2 + 2\bar{n}(2+\bar{n})U^2}{\bar{n}(2-\bar{n})(32t_h^2 + \bar{n}(2-\bar{n})U^2)} \tag{S16}$$

$$s_{ne} = \frac{8\bar{n}U}{\bar{n}(2-\bar{n})(32t_h^2 + \bar{n}(2-\bar{n})U^2)}. \tag{S17}$$

For the experimental parameters $\bar{n} = 0.6$ and $U/t_h = 3.9$ these coefficients take the values $s_{nn} \approx 2.96$, $s_{ee} \approx 0.43$, $s_{ne} \approx 0.50$ in units where $t_h = 1$.

## Simultaneous fitting of the model

As explained in the previous sections, there is a fast and a slow exponential decay solution to our hydrodynamic model. In the strong tilt regime, Eqn. S9 shows that the slow decay depends only on the thermal diffusivity $D_{\mathrm{th}}$.

We perform a simultaneous fit to all wavelengths at a given tilt strength as explained in the supplement of [2]. The fitting function is

$$A(t) = A_0 e^{-\Gamma_-(D_{\mathrm{th}},F,k)t}, \tag{S18}$$

and it is fitted only to the late-time decay. Here, $A_0$ is a fitting parameter that can vary for each wavelength while $D_{\mathrm{th}}$ is fitted globally to all wavelengths. The parameters $F$ and $k$ are fixed according to our experimentally measured values. The results of fitting this model to measurements in the strong tilt regime are shown in Fig. S4.

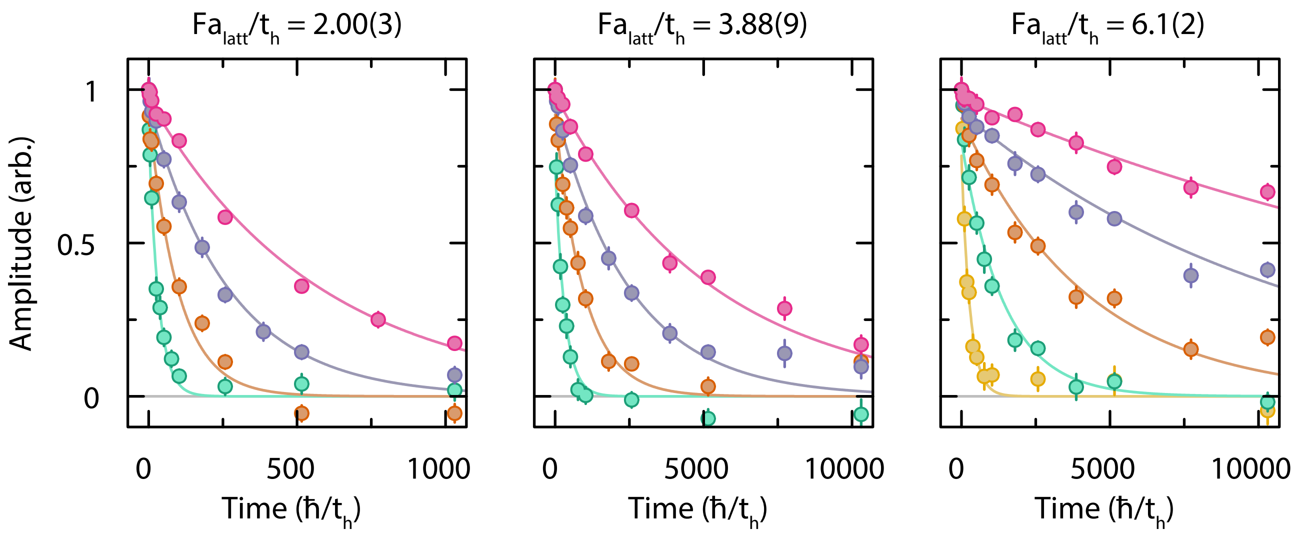


FIG. S4. **Simultaneous fitting of hydrodynamic model.** Fitted normalized relative amplitudes of the periodic density modulation (circles) *vs.* time for wavelengths 7.69(3) $a_{\rm latt}$ (yellow), 11.46(3) $a_{\rm latt}$ (green), 15.16(5) $a_{\rm latt}$ (orange), 19.33(7) $a_{\rm latt}$ (purple), and 23.3(2) $a_{\rm latt}$ (pink) at different tilts. The lines are simultaneous fits of the hydrodynamic model to the long-time decay after the initial average heating (phase change). We are able to extract the thermal diffusivity through this fitting method.


[1] Peter T. Brown, Debayan Mitra, Elmer Guardado-Sanchez, Peter Schauß, Stanimir S. Kondov, Ehsan Khatami, Thereza Paiva, Nandini Trivedi, David A. Huse, and Waseem S. Bakr, "Spin-imbalance in a 2D Fermi-Hubbard system," Science **357**, 1385–1388 (2017).

[2] Peter T. Brown, Debayan Mitra, Elmer Guardado-Sanchez, Reza Nourafkan, Alexis Reymbaut, Charles-David Hébert, Simon Bergeron, A.-M. S. Tremblay, Jure Kokalj, David A. Huse, Peter Schauß, and Waseem S. Bakr, "Bad metallic transport in a cold atom Fermi-Hubbard system," Science **363**, 379–382 (2019).

[3] Philipp M. Preiss, Ruichao Ma, M. Eric Tai, Alexander Lukin, Matthew Rispoli, Philip Zupancic, Yoav Lahini, Rajibul Islam, and Markus Greiner, "Strongly correlated quantum walks in optical lattices," Science **347**, 1229–1233 (2015).

[4] Ruichao Ma, M. Eric Tai, Philipp M. Preiss, Waseem S. Bakr, Jonathan Simon, and Markus Greiner, "Photon-assisted tunneling in a biased strongly correlated Bose gas," Phys. Rev. Lett. **107**, 095301 (2011).